

## JGR Atmospheres

## RESEARCH ARTICLE

10.1029/2018JD030148

## Shrinkage of East Asia Winter Monsoon Associated With Increased ENSO Events Since the Mid-Holocene

J. Wu<sup>1,2</sup> , Q. Liu<sup>1,2</sup>, Q. Y. Cui<sup>3</sup> , D. K. Xu<sup>1,2,4</sup>, L. Wang<sup>1,2</sup> , C. M. Shen<sup>5</sup> , G. Q. Chu<sup>1,2,6</sup> , and J. Q. Liu<sup>1,7</sup>

## Key Points:

- A pollen record from Lake Moon in Northeast China in Holocene implies the shrinkage of the EAWM after 6 ka BP
- The teleconnection between the EAWM and El Niño events is obvious in Holocene
- Solar activity may be main driving force of the ENSO and the EAWM on centennial/millennial time scale since mid-Holocene

## Supporting Information:

- Supporting Information S1
- Table S1

## Correspondence to:

J. Wu and J. Q. Liu,  
wujing@mail.iggcas.ac.cn;  
liujq@mail.iggcas.ac.cn

## Citation:

Wu, J., Liu, Q., Cui, Q. Y., Xu, D. K., Wang, L., Shen, C. M., et al. (2019). Shrinkage of East Asia winter monsoon associated with increased ENSO events since the mid-Holocene. *Journal of Geophysical Research: Atmospheres*, 124, 3839–3848. <https://doi.org/10.1029/2018JD030148>

Received 14 DEC 2018

Accepted 15 MAR 2019

Accepted article online 27 MAR 2019

Published online 4 APR 2019

## Author Contributions:

Funding acquisition: Q. Liu, J. Q. Liu

Investigation: Q. Liu, J. Q. Liu

Project administration: Q. Liu, J. Q. Liu

Software: Q. Y. Cui, D. K. Xu, G. Q. Chu

Writing - original draft: Q. Y. Cui, L. Wang, J. Q. Liu

Writing - review &amp; editing: Q. Y. Cui, D. K. Xu, L. Wang, C. M. Shen, G. Q. Chu

<sup>1</sup>Key Laboratory of Cenozoic Geology and Environment, Institute of Geology and Geophysics, Chinese Academy of Sciences, Beijing, China, <sup>2</sup>Institutions of Earth Science, Chinese Academy of Sciences, Beijing, China, <sup>3</sup>Key Laboratory of Land Surface Pattern and Simulation, Institute of Geographical Sciences and Natural Resources Research, Chinese Academy of Sciences, Beijing, China, <sup>4</sup>Center for Excellence in Tibetan Plateau Earth Sciences, CAS, Beijing, China, <sup>5</sup>Key Laboratory of Plateau Lake Ecology and Global Change, Yunnan Normal University, Kunming, China, <sup>6</sup>Center for Excellence in Life and Paleoenvironment, CAS, Beijing, China, <sup>7</sup>College of Earth and Planetary Sciences, University of Chinese Academy of Sciences, Beijing, China

**Abstract** Instrumental records indicate a close relationship between the El Niño-Southern Oscillation and the East Asian winter monsoon (EAWM) on interannual to decadal time scales. However, few studies have examined possible links between them on centennial/millennial time scales. In Northeast China, modern observations show that the immigration of temperate forest trees such as *Pinus* (pine) and *Quercus* (oak) into cold temperate boreal forest is sensitive to changes in winter temperature. Here we present a continuous high-resolution pollen record from Lake Moon in the central part of the Great Khingan Mountain Range, Northeast China. The record reveals increasing contents of *Pinus* and *Quercus* pollen after ~6.0 ka cal. BP, which may indicate a gradual weakening of the EAWM. It is broadly coupled with an increasing El Niño frequency since the middle Holocene, and we observe a statistically significant correlation between the percentages of *Pinus* and *Quercus* and a time series of El Niño events. On the centennial to millennial time scale, the results of wavelet analysis and band-pass filtering show that the occurrence and development of El Niño have also promoted a weaker EAWM after ~6.0 ka cal. BP, which is inversely correlated with the variation of the ca. 500-year cycle originated from changes in solar output. These results imply that the climate transition in the mid-Holocene is caused by the change of variations in solar activity and amplified by ocean circulation El Niño-Southern Oscillation to influence the East Asian Monsoon system, especially the EAWM, and finally change the vegetation in Great Khingan Mountain Range.

## 1. Introduction

The East Asian winter monsoon (EAWM) is the most active and powerful atmospheric circulation system during the Northern Hemisphere winter. The EAWM has large environmental, societal, and economic impacts in its region of influence due to the associated severe cold surges and heavy snowfall. In addition to regional impacts, the EAWM may have a global impact through its effects on the Walker circulation. Previous studies have indicated that the EAWM and the El Niño-Southern Oscillation (ENSO) are tightly coupled (An et al., 2017; Cheung et al., 2012; Li, 1990; Li et al., 2005; Wen et al., 2000; Zhou et al., 2007). The ENSO is the abnormal sea surface warming or cooling phenomena affected the globe climate change, whose main center located over the tropical Pacific Ocean (An et al., 2017; Cheung et al., 2012). Generally, an El Niño event weakens the EAWM leading to a positive surface temperature anomaly across most parts of China through changes in anticyclonic circulation over the northwestern Pacific during the boreal winter, which is reversed in La Niña years (Cheung et al., 2012; Li, 1990; Wen et al., 2000). On the other hand, a stronger (weaker) EAWM promotes the occurrence and development of El Niño (La Niña) events (Li et al., 2005; Zhou et al., 2007).

On the interdecadal to decadal time scale, meteorological observations indicate a significant correlation between ENSO and EAWM (He & Wang, 2013; Kim et al., 2016; Wang et al., 2012). Much effort has been made to understand the long-term variability of the EASM using records from loess-paleosol sequences (e.g., Ding et al., 1995; Sun et al., 2010; Xiao et al., 1995), lacustrine sediments (e.g., Liu et al., 2009; Wang et al., 2012), stalagmites (Sone et al., 2013), and marine sediments (e.g., Huang et al., 2011; Steinke et al.,

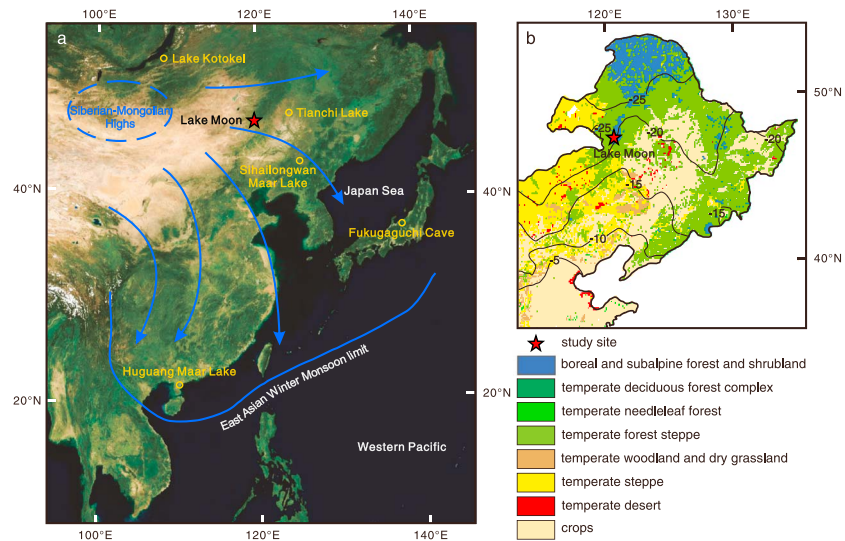


**Figure 1.** Location of Lake Moon. (a) Location of the study site and other paleoclimatic records mentioned in the text. The trajectory of the East Asian winter monsoon is indicated by blue arrows; (b) distribution of vegetation within the study region in Northeast China (Wang et al., 2013); winter temperature contours are in degrees Celsius.

2011 ; Yamamoto et al., 2013). On longer time scales, however, only a few studies have examined possible links between ENSO and the EAWM based on climate model simulations and sediment records from low latitude regions (An et al., 2017; Xu et al., 2009; Zheng et al., 2014). In addition, there is a distinct lack of records from the most active region of the EAWM such as the midhigh latitudes of continental Asia.

The distribution of modern vegetation in Northeast China is significantly influenced by winter temperatures; for example, the boundary between the boreal forest and temperate deciduous forest, such as on the eastern margin of the Great Khingan Mountain Range, is largely determined by winter temperature (Du et al., 2011). Here we present a winter-temperature-sensitive pollen record from a Holocene lake sediment core from Lake Moon, Northeast China. We use the record to reconstruct the evolution of the EAWM in the Holocene and to investigate the teleconnection between the EAWM and the ENSO on centennial/millennial time scales.

## 2. Materials and Methods

### 2.1. Study Site

Lake Moon (47°30.36'N, 120°51.99'E, 1,190 m above sea level) is in the Arxan-Chaihe volcanic field in the central part of the Great Khingan Mountain Range (Figure 1), 33 km from Chaihe Town, Zhalantun City, Inner Mongolia. The lake is a crater lake located in a scoria cone (Sun et al., 2017), whose surface area is ~0.03 km<sup>2</sup>, the maximum water depth is 6.5 m, and there is no inflow or outflow. The annual precipitation is ~300–600 mm, and the mean annual temperature is –4–0 °C with extremely low temperatures in January, from –32 to –20 °C. The vegetation surrounding Lake Moon is boreal deciduous broadleaf-conifer mixed forest, dominated by *Larix gmelinii* (Dahurian larch), *Betula platyphylla* (Siberian silver birch), and *B. dahurica* (Asian black birch), which can resist the long cold winter.

### 2.2. Sediment Cores and Chronology

An 886-cm sedimentary sequence, comprising three overlapping piston cores, was obtained from the center of Lake Moon in March 2007. The chronology of the core is based on 21 AMS <sup>14</sup>C dates from terrestrial and aquatic plant macrofossils and bulk sediment; the dating was conducted at Poznan Radiocarbon Laboratory (Liu et al., 2010; Wu et al., 2016; Wu & Liu, 2012; see supporting information Table S1). The lithology of the upper 544 cm consists of dark-brown finely laminated gyttja in Holocene. In this study, a new age-depth model is established by Bacon V2.2 (Blaauw & Christen, 2011), a Bayesian approach based on all the radiocarbon ages previously published (see Figure S1).

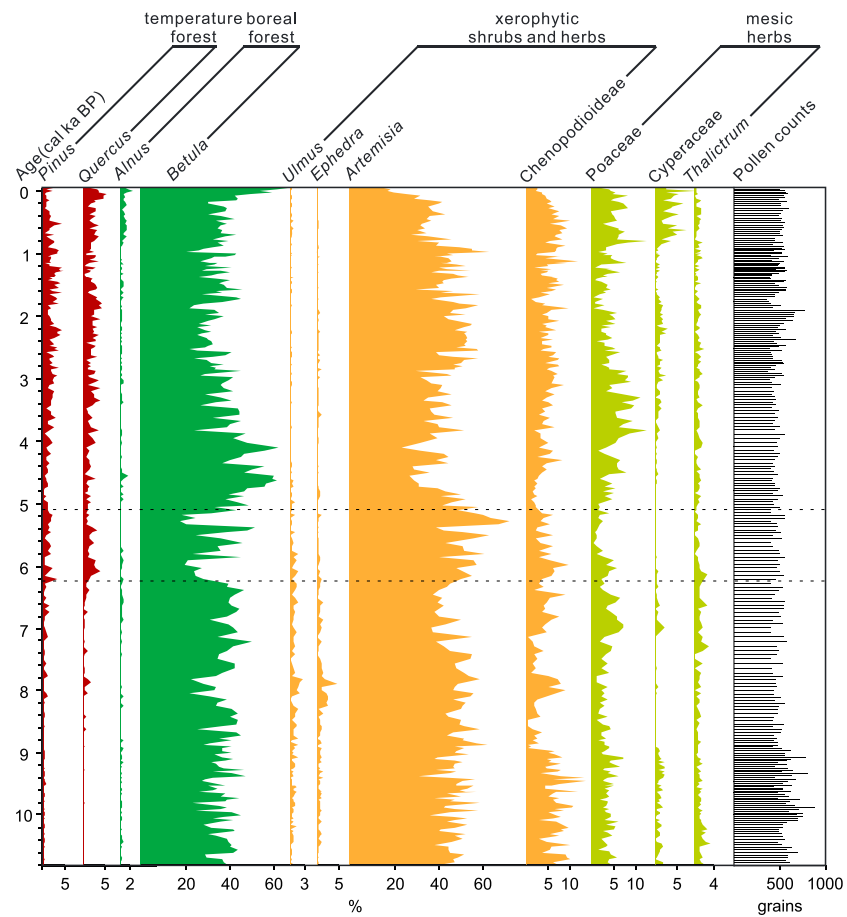


Figure 2. Simplified pollen percentage diagram for Lake Moon.

### 2.3. Methods

#### 2.3.1. Pollen Analysis

Pollen analysis was conducted at a 2-cm interval. The samples were prepared using standing alkali and acid treatments (Moore et al., 1991). Pollen grains were identified using an optical microscope at 400X magnification with the aid of pollen atlases and keys (Wang et al., 1995; Wang & Wang, 1983). More than 400 terrestrial pollen grains were counted for most samples. Pollen percentages for each taxon were calculated using the sum of terrestrial pollen grains. In addition to the previously published pollen data (Wu & Liu, 2012), we got new data from the upper 50 cm of the sequence to obtain the pollen record from the Lake Moon spanning the Holocene.

#### 2.3.2. Data Analysis

Spearman rank correlation coefficients (Press et al., 1992) were used to examine the relationship between variations in the frequencies of tree pollen taxa especially sensitive to the EAWM (*Pinus* and *Quercus*) and a time series of ENSO events. Non-parametric statistics were chosen because the data sets do not exhibit Gaussian distributions. As the calculation of Spearman rank correlation coefficients could only be performed between records with the same resolution, the percentages of the *Pinus* and *Quercus* records and ENSO records resampled at a 20-year resolution based on interpolation. In addition, wavelet analysis (Torrence & Compo, 1998) of the *Pinus* and *Quercus* records was used to provide a simultaneous representation of the data in the time and frequency domains and thus to investigate the possible localization of cyclic patterns. Prior to the wavelet analysis, the *Pinus* and *Quercus* time series were resampled at a 10-year resolution based on interpolation and filtered to remove false cycles. The wavelet analysis was conducted using wavelet package in Matlab software.

### 3. Results and Discussion

#### 3.1. Pollen Records

Two hundred seventy-two pollen samples were analyzed, spanning the last 10.8 cal ka BP, with an average time resolution was 40 a. A simplified pollen diagram for Lake Moon is presented in Figure 2, whose data are available from Table S2. The pollen spectra can be grouped into the following vegetation categories: cold temperate boreal forest, temperate forest, mesic herbs, and xerophytic shrubs and herbs. Cold temperate boreal forest taxa mainly comprise *Betula* and *Alnus*, while the temperate forest taxa include *Pinus* and *Quercus*. Mesic herbs mainly comprise Poaceae, Cyperaceae, and *Thalictrum*. Xerophytic shrubs and herbs comprise *Artemisia*, Chenopodioideae (Chenopodiaceae), *Ulmus*, and *Ephedra*. The pollen record indicates that the vegetation in the central part of the Great Khingan Mountain Range was forest-steppe throughout the Holocene. Nonetheless, there are significant changes in the proportions of the taxa representing the four groups of plant communities described above, the most prominent of which is the significantly higher frequencies of *Pinus* and *Quercus* since ca. 6.0 ka cal BP (Figure 2) compared to their extremely low representation in the early Holocene.

#### 3.2. Proxies of the EAWM

Previous studies have shown that broad-leaved deciduous taxa, such as *Betula*, and boreal forest taxa, such as *Larix*, have a high degree of cold tolerance (Prentice et al., 1992; Sakai, 1979; Sakai & Weiser, 1973). In the present study area, the modern vegetation, that is, deciduous broadleaf-conifer mixed forest dominated by *Larix gmelinii* and *Betula* spp., is habituated to the long and cold winter (for reference, from 1946 to 1999, there were 85 days altogether with a daily minimum air temperature of less than  $-40^{\circ}\text{C}$  at the study site, www.hadobs.org). In contrast, temperate forest trees such as *Pinus* and *Quercus*, which are only sporadically present in the Great Khingan Mountain Range at the present day, are damaged by spontaneous ice nucleation below  $-40^{\circ}\text{C}$  (Sakai & Weiser, 1973); thus, the winter temperature is a crucial limiting factor for their survival in midhigh latitude regions. Therefore, the immigration of *Pinus* and *Quercus* into the cold temperate boreal forest represents an increase in the winter temperature and is linked to the weakening of the EAWM. The extension of *Pinus* and *Quercus* is not only recorded at Lake Moon but also in other lake sediment records from the midhigh latitude region of the Far East after 6.0 ka cal BP, for example, at Tianchi Lake, Sihailongwan Maar Lake, Lake Kolotel (Figures 1 and 3c–3f) and Jinchuan peat bog (Jiang et al., 2008; Stebich et al., 2015; Tarasov et al., 2009; Zhou et al., 2016). The contents of *Pinus* and *Quercus* in pollen assemblages at these sites are also likely to be inversely correlated with the strength of the EAWM.

The trends in *Pinus* and *Quercus* at Lake Moon are synchronous with other EAWM indicators from low latitudes in the East Asian Monsoon (EAM) region, such as at Fukugaguchi Cave (Sone et al., 2013; Figure 3g) and Huguang Maar Lake (Wang et al., 2012; Figure 3h). This synchronous behavior clearly demonstrates a weakening of the EAWM at  $\sim 6.0$  ka cal BP, confirming the reliability of the pollen proxies as an indicator of the EAWM, and indicating a teleconnection of climate change in midhigh latitudes and low latitudes of the EAM region.

#### 3.3. Factors of the EAWM Weakening Since Mid-Holocene

The increasing percentages of *Pinus* and *Quercus* at Lake Moon clearly demonstrate the weakening of the EAWM since  $\sim 6.0$  ka cal BP. This trend is consistent with that of increasing winter (December–January–February) insolation at the latitude of study site throughout the entire Holocene (Berger & Loutre, 1991; Figure 4a; black line), which provides a partial explanation for the warmer winter temperatures in Northeast China after  $\sim 6.0$  ka cal BP.

Second, the sea surface temperature (SST) of the western tropical Pacific Ocean could also affect the intensity of the EAWM. The SST in the western tropical Pacific Ocean has dropped  $\sim 0.5^{\circ}\text{C}$  over the past 10.0 ka BP (Stott et al., 2004; Figure 4c; dark blue line). The cooling SST would reduce the land-sea thermal contrast between Pacific and Siberian air masses in winter, which weaken the strength of the EAWM under the assumption of constant Siberian high.

However, the relatively gradual changes in winter insolation and the SST of the western tropical Pacific Ocean cannot entirely explain the relatively abrupt weakening of the EAWM at 6–5 ka cal BP represented from this study, Huguang Maar Lake (Wang et al., 2012) and Fukugaguchi Cave (Sone et al., 2013). Thus,

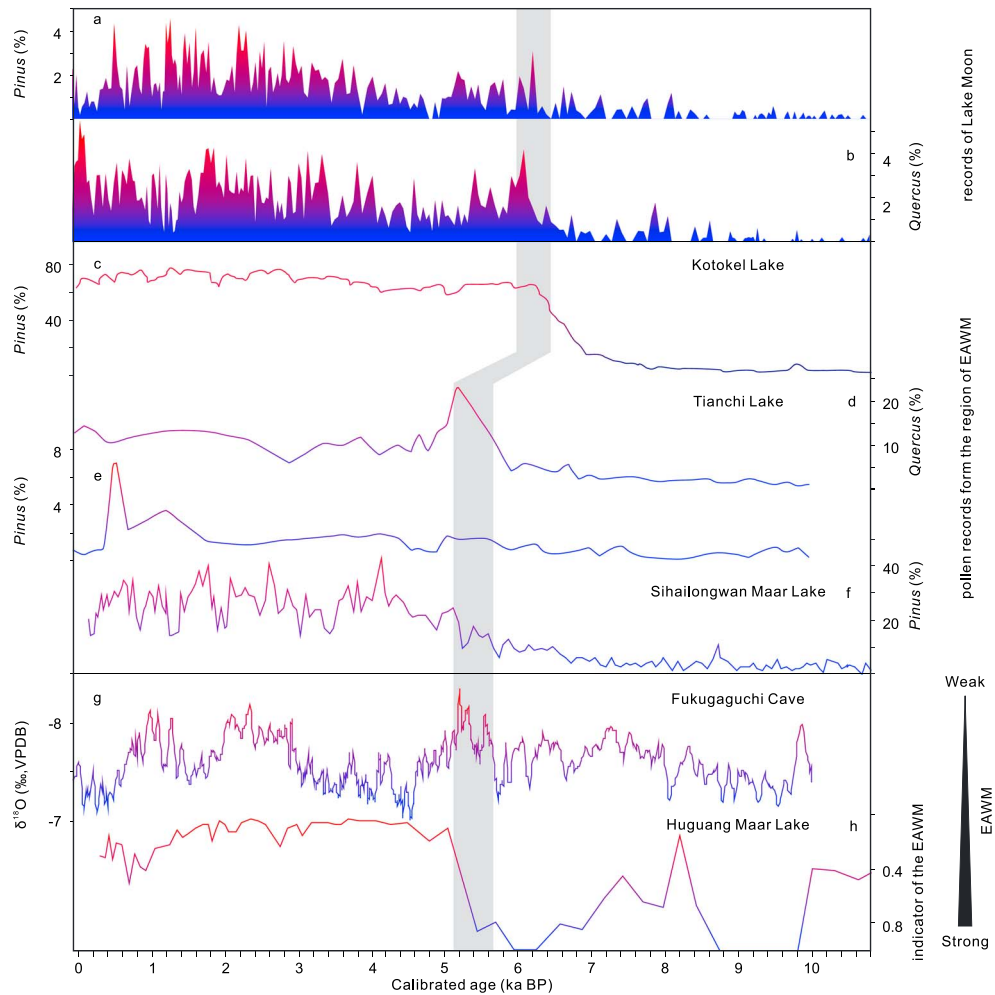


**Figure 3.** Time series of *Pinus* and *Quercus* frequencies at Lake Moon and other lake sites in midhigh latitudes of the East Asian Monsoon region compared with other EAWM proxies from the East Asian Monsoon region. (a and b) Records of *Pinus* and *Quercus* from Lake Moon (this study); (c) *Pinus* record from Lake Kotokel (Tarasov et al., 2009); (d and e) records of *Quercus* and *Pinus* from Tianchi Lake (Zhou et al., 2016); (f) *Pinus* record from Sihailongwan Maar Lake (Stebich et al., 2015); (g)  $\delta^{18}\text{O}$  record ( $\text{‰}$ , VPDB (Vienna Pee Dee Belemnite); 5-point running average) from Fukugaguchi Cave (Sone et al., 2013); (h) EAWM indicator from Huguang Maar lake (Wang et al., 2012). EAWM = East Asian winter monsoon.

other potential factors, like ENSO variability on centennial/millennial time scales, need to be considered (Figure 4b; Cobb & Charles, 2013; Moy et al., 2002). The results of Spearman rank correlation between 11 major pollen taxa from Lake Moon and two time series of ENSO events from the Laguna Pallcacocha, Ecuador (Moy et al., 2002) and the Northern Line Islands (Cobb & Charles, 2013) were presented in Table 1. Higher correlation coefficients (0.616, 0.619, 0.426, and 0.418) imply highly significant relationships between percentages of *Pinus* and *Quercus* and frequencies of El Niño events. These results reveal a relatively strong relationship between the EAWM and ENSO events on centennial/millennial time scales.

### 3.4. Approximately 500-Year Cycles of the EAWM

In this study, the results of wavelet analysis and band-pass filtering of the *Pinus* and *Quercus* records from Lake Moon are illustrated in Figure 5. The results show a period of low variance (blue and green colors) from 10.8 to 6.0 ka cal BP and a period of high variance (yellow and red colors) after ~6.0 ka cal BP (Figures 5a, 5c, and 5e). A prominent feature of the wavelet analysis is that a ~500-year quasiperiodic component exhibits stronger variance after ~6.0 ka cal BP (Figures 5a and 5c), and a 400–600-year band-pass filter of the data reveals the same phenomenon (Figures 5b and 5d). These results indicate that ca. 500-year cycle exists in the intensity change of the EAWM. A similar periodicity has been noted previously in other Holocene

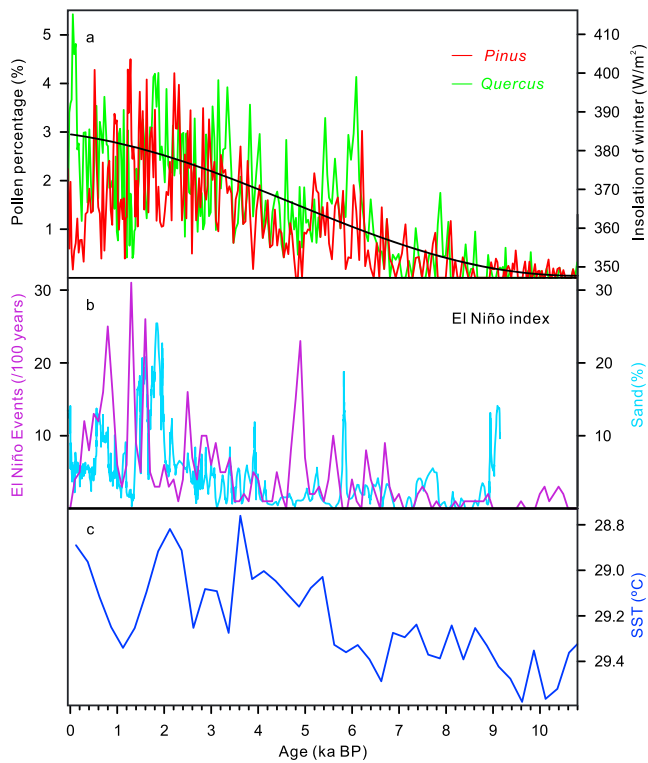


**Figure 4.** Comparison between the pollen records from Lake Moon with winter insolation at 45°N, two El Niño-Southern Oscillation indices and SST of the western tropical Pacific Ocean. (a) Pollen records of *Pinus* (red line) and *Quercus* (green line) from Lake Moon and winter insolation at 45°N from Berger and Loutre (1991; black line); (b) El Niño-Southern Oscillation indices recorded by the lacustrine sediment from the Laguna Pallcacocha from Moy et al. (2002) (purple line) and the fossil coral records from the Northern Line Islands from Cobb and Charles (2013; light blue line); (c) SST recorded by the oxygen isotope and Mg/Ca data from foraminifers in the western tropical Pacific Ocean from Stott et al. (2004; dark blue line). SST = sea surface temperature.

**Table 1**

*Spearman Rank Correlation Coefficients for Two El Niño-Southern Oscillation Indices (Cobb & Charles, 2013; Moy et al., 2002) and the Frequencies of Major Pollen Taxa at Lake Moon (20-year Resolution)*

| Spearman rank correlation | El Niño event (Moy et al., 2002) | Sand % (Cobb & Charles, 2013) |
|---------------------------|----------------------------------|-------------------------------|
| <i>Pinus</i> (%)          | <b>0.616</b>                     | <b>0.426</b>                  |
| <i>Quercus</i> (%)        | <b>0.619</b>                     | <b>0.418</b>                  |
| <i>Alnus</i> (%)          | <b>0.262</b>                     | <b>0.313</b>                  |
| <i>Betula</i> (%)         | -0.001                           | -0.229                        |
| <i>Ulmus</i> (%)          | -0.439                           | -0.365                        |
| <i>Ephedra</i> (%)        | -0.498                           | -0.285                        |
| <i>Artemisia</i> (%)      | -0.223                           | -0.076                        |
| Chenopodiaceae (%)        | 0.032                            | <b>0.329</b>                  |
| Poaceae (%)               | <b>0.167</b>                     | <b>0.177</b>                  |
| Cyperaceae (%)            | <b>0.143</b>                     | <b>0.507</b>                  |
| <i>Thalictrum</i> (%)     | -0.188                           | -0.082                        |

Note. Bold indicates significant at the 0.1% level.

paleoclimate records from Northeast China, including plant cellulose in peat deposits (Hong et al., 2001) and pollen records from maar lakes in Longgang Volcanic Field (Stebich et al., 2015; Xu et al., 2014). This periodicity is evident in the proxy records of the EASM including summer temperature and rainfall; in this study it is also evident in a record of the EAWM.

The wavelet analysis and the band-pass filter of the frequencies of El Niño events recorded in the sedimentation from Laguna Pallcacocha, Ecuador (Figures 5e and 5f; Moy et al., 2002), also present similar results with the proxies of the EAWM that a ~500-year quasiperiodic component exhibits stronger variance after ~6.0 ka cal BP (Figures 5e and 5f). All these results indicate that the variance of ca. 500-year cycle becomes greater both in the intensity change of the EAWM and the frequencies of the ENSO events after ~6.0 ka cal BP.

Ca. 500-year cycle originates from changes in solar output (Steinhilber et al., 2012; Stuiver et al., 1995), which affects the dynamics of atmospheric and oceanic processes (Chapman & Shackleton, 2000; Cheng et al., 2016; Wang et al., 2005; Zhu et al., 2017). The amplitude of variation of ~500-year quasiperiodic component of solar output before ~6 ka cal BP is greater than that after, which was not detected in the climate records in Northeast China in early Holocene in previous and this study (Stebich et al., 2015; Xu et al., 2014). This phenomenon indicates that the EAM system is closely linked to the high-latitudes processes in early Holocene, mainly the global ice volumes, while the impacting of the tropical teleconnection between ENSO and the EAM system becomes more significant during the midlate Holocene with the decreased global ice volumes (Wang et al., 2012). The anomalous anticyclone located in the western North Pacific has existed since ~6 ka cal BP as the bridge between ENSO and the EAWM, which is joint with strong southerly winds along the East Asian coasts weakened the EAWM significantly (Wang et al., 2000; Wang et al., 2012). On these views, it is believed that the variation of solar output makes the weakening of the Walker circulation, the increasing of El Niño events, and the shrinkage of the EAWM since the mid-Holocene. This transition is synchronous with the onset of the “modern” ENSO (Moy et al., 2002; Sandweiss et al., 2001) and also is widely acknowledged globally in the mid-Holocene (Mayewski et al., 2004; Steig, 1999) as the termination of the Holocene thermal maximum, the hemispheric even global cooling, drier conditions in central to eastern Asia and Africa under the abrupt weakening of the monsoonal system, wetter conditions in northern Europe and southern South America (Magny et al., 2006; Roland et al., 2015; Zhou et al., 2016). The synchronicity of all these transitions implies that a reorganization in the Earth’s ocean-atmosphere circulation system occurred in the mid-Holocene. This global event was ascribed to variations in solar activity, orbitally driven insolation changes (Hodell et al., 2001; Magny & Haas, 2004; Mayewski et al., 2004; Wanner et al., 2008) or nonlinear feedback processes within the climate system components, especially changes in ocean circulation (e.g., NAO (North Atlantic oscillation), ITCZ (intertropical convergence zone), and ENSO; Holmes et al., 2011; Schneider, 2004; Wunsch, 2006). Based on this study, the climate transition in the mid-Holocene is caused by the variations in solar activity and amplified by ocean circulation ENSO to influence the EAM system and then change the vegetation in Great Khingnan Mountain Range, Northeast China.

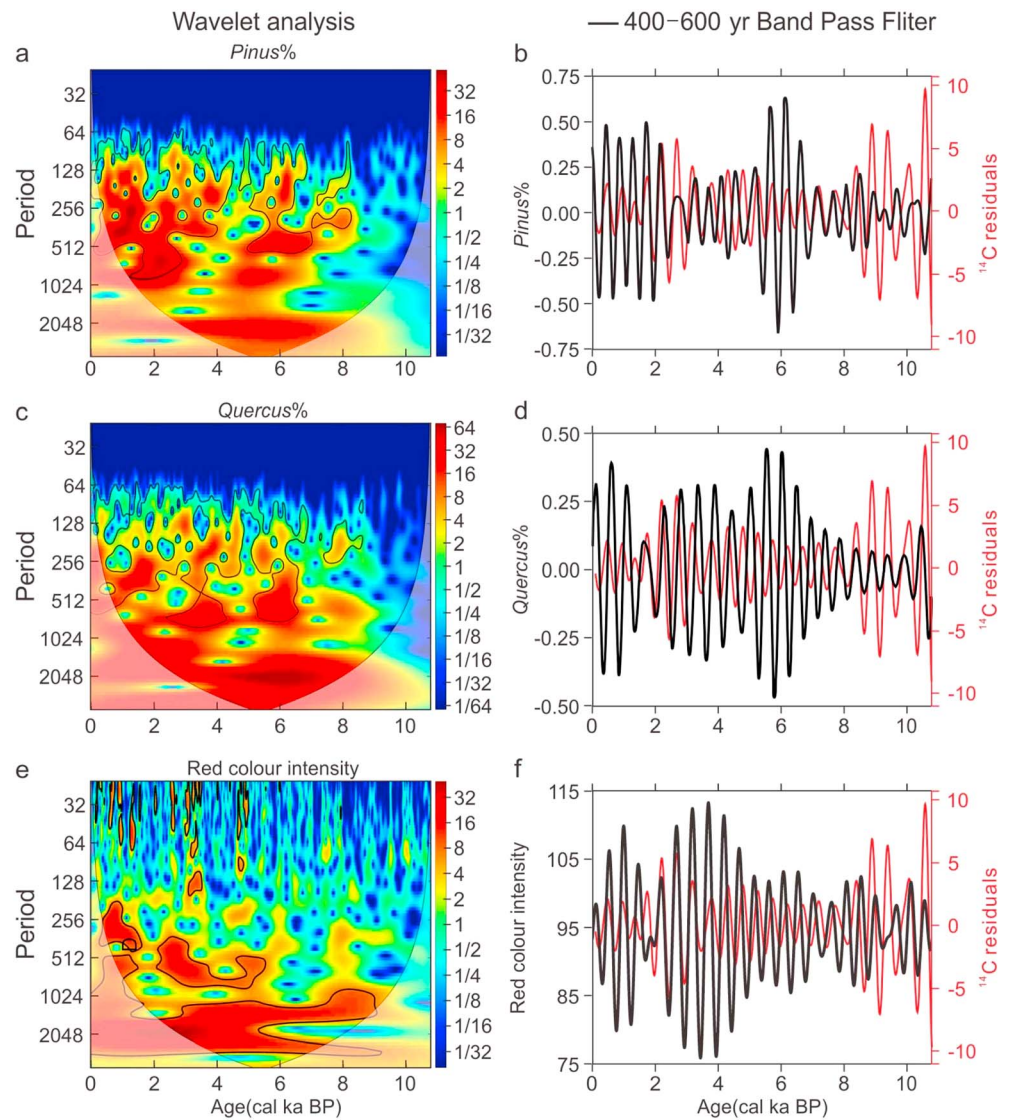


**Figure 5.** Wavelet spectrum and band-pass filtering calculated on pollen records and El Niño-Southern Oscillation index. (a–d) Results of wavelet spectrum and band-pass filtering calculated on *Pinus* (%) and *Quercus* (%) record from Lake Moon; (e and f) results of wavelet spectrum and band-pass filtering calculated on red color intensity record from the Laguna Pallcacocha from Moy et al. (2002); the red line (b, d, and f) is the results of the band-pass filtering calculated on the  $\delta^{14}\text{C}$  residuals indicated the change of solar output (Stuiver et al., 1998). The wavelet power spectra for *Pinus* and *Quercus* were obtained after interpolation to evenly spaced data. The shape of the mother wavelet was set to Morlet. High (low) power is indicated by red (blue) color. High power can reach 32 or 64 values, while low power can be as low as 1/32 or 1/64 values. The 5% significance level against red noise is shown as a thick contour. The dark shaded area indicates the cone-of-influence, where edge effects become significant. This means the result of this area is unreliable.

#### 4. Conclusions

We have obtained a time series of warm winter events since 10.8 cal ka BP based on the changes in the frequencies of *Pinus* and *Quercus* pollen in the sediments of Lake Moon, in Northeast China. The data provide a robust record of changes in EAWM intensity in the midhigh latitude region of the EAM, and it extends the time scale of a teleconnection between El Niño events and the EAWM from interannual/interdecadal to centennial/millennial.

The results of correlation analysis indicate that the EAWM weakened after 6.0 cal ka BP which was also related to the frequency of El Niño events on centennial/millennial time scales. Furthermore, the

enhancement of El Niño events was the result of the increased prominence of the ~500-year cycle in solar output during the mid-Holocene.

Based on the results from this study, the climate transition in the mid-Holocene is caused by the variations in solar activity and amplified by ocean circulation ENSO to influence the intensity of the EAWM and change the vegetation in Great Khingan Mountain Range, Northeast China.

#### Acknowledgments

This work was supported by the National Natural Science Foundation of China (41572353, 41320104006, and 41561144010) and Yunnan project for the introduction of advanced talents (2013HA024). We would like to thank Alan Sandford Palmer as well as another anonymous reviewer for their constructive comments and suggestions. The pollen data from Lake Moon in Holocene are available from Table S2.

#### References

- An, S.-I., Kim, H.-J., Park, W., & Schneider, B. (2017). Impact of ENSO on East Asian winter monsoon during interglacial periods: Effect of orbital forcing. *Climate Dynamics*, *49*(9-10), 3209–3219. <https://doi.org/10.1007/s00382-016-3506-8>
- Berger, A., & Loutre, M. F. (1991). Insolation values for the climate of the last 10 million years. *Quaternary Science Reviews*, *10*(4), 297–317. [https://doi.org/10.1016/0277-3791\(91\)90033-Q](https://doi.org/10.1016/0277-3791(91)90033-Q)
- Blaauw, M., & Christen, J. A. (2011). Flexible paleoclimate age-depth models using an autoregressive gamma process. *Bayesian Analysis*, *6*(3), 457–474.
- Chapman, M. R., & Shackleton, N. J. (2000). Evidence of 550-year and 1000-year cyclicities in North Atlantic circulation patterns during the Holocene. *Holocene*, *10*(3), 287–291. <https://doi.org/10.1191/095968300671253196>
- Cheng, H., Sinha, A., Verheyden, S., Nader, F. H., Li, X. L., Zhang, P. Z., et al. (2016). The climate variability in northern Levant over the past 20,000 years. *Geophysical Research Letters*, *42*, 8641–8650. <https://doi.org/10.1002/2015GL065397>
- Cheung, H. N., Zhou, W., Mok, H. Y., & Wu, M. C. (2012). Relationship between Ural-Siberian blocking and the East Asian winter monsoon in relation to the Arctic Oscillation and the El Niño-Southern Oscillation. *Journal of Climate*, *25*(12), 4242–4257. <https://doi.org/10.1175/JCLI-D-11-00225.1>
- Cobb, K. M., & Charles, C. D. (2013). Highly variable El Niño-Southern Oscillation throughout the Holocene. *Science*, *339*(6115), 67–70. <https://doi.org/10.1126/science.1228246>
- Ding, Z., Liu, T., Rutter, N. W., Yu, Z., Guo, Z., & Zhu, R. (1995). Ice-volume forcing of East Asian winter monsoon variations in the past 800,000 years. *Quaternary Research*, *44*(02), 149–159. <https://doi.org/10.1006/qres.1995.1059>
- Du, H., Wu, Z., & Li, M. (2011). Interdecadal changes of vegetation transition zones and their responses to climate in Northeast China. *Theoretical and Applied Climatology*, *106*(1-2), 179–188. <https://doi.org/10.1007/s00704-011-0432-x>
- He, S., & Wang, H. (2013). Oscillating relationship between the East Asian winter monsoon and ENSO. *Journal of Climate*, *26*(24), 9819–9838. <https://doi.org/10.1175/JCLI-D-13-00174.1>
- Hodell, D. A., Kanfoush, S. L., Shemesh, A., Crosta, X., Charles, C. D., & Guilderson, T. P. (2001). Abrupt cooling of Antarctic surface waters and sea ice expansion in the South Atlantic sector of the Southern Ocean at 5000 cal yr B.P. *Quaternary Research*, *56*(02), 191–198. <https://doi.org/10.1006/qres.2001.2252>
- Holmes, J., Lowe, J., Wolff, E., & Srokosz, M. (2011). Rapid climate change: Lessons from the recent geological past. *Global and Planetary Change*, *79*(3-4), 157–162. <https://doi.org/10.1016/j.gloplacha.2010.10.005>
- Hong, Y. T., Wang, Z. G., Jiang, H. B., Lin, Q. H., Hong, B., Zhu, Y. X., et al. (2001). A 6000-year record of changes in drought and precipitation in northeastern China based on a  $\delta^{13}C$  time series from peat cellulose. *Earth and Planetary Science Letters*, *185*(1-2), 111–119. [https://doi.org/10.1016/S0012-821X\(00\)00367-8](https://doi.org/10.1016/S0012-821X(00)00367-8)
- Huang, E., Tian, J., & Steinke, S. (2011). Millennial-scale dynamics of the winter cold tongue in the southern South China Sea over the past 26 ka and the East Asian winter monsoon. *Quaternary Research*, *75*(01), 196–204. <http://doi.org/10.1016/j.yqres.2010.08.014>
- Jiang, W., Leroy, S. A. G., Ogle, N., Chu, G., Wang, L., & Liu, J. (2008). Natural and anthropogenic forest fires recorded in the Holocene pollen record from a Jinchuan peat bog, northeastern China. *Palaeogeography, Palaeoclimatology, Palaeoecology*, *261*(1-2), 47–57. <https://doi.org/10.1016/j.palaeo.2008.01.007>
- Kim, J.-W., An, S.-I., Jun, S.-Y., Park, H.-J., & Yeh, S.-W. (2016). ENSO and East Asian winter monsoon relationship modulation associated with the anomalous Northwest Pacific anticyclone. *Climate Dynamics*, *49*(4), 1157–1179. <https://doi.org/10.1007/s00382-016-3371-5>
- Li, C. (1990). Interaction between anomalous winter monsoon in East Asia and El Niño events. *Advances in Atmospheric Sciences*, *7*(1), 36–46.
- Li, C., Pei, S., & Pu, Y. (2005). Dynamical impact of anomalous East-Asian winter monsoon on zonal wind over the equatorial western Pacific. *Chinese Science Bulletin*, *50*(14), 1520–1526. <https://doi.org/10.1360/04wd0327>
- Liu, Q., Li, Q., Wang, L., & Chu, G. Q. (2010). Stable carbon isotope record of bulk organic matter from a sediment core at Moon Lake in the middle part of Daxing'an Mountain range in Northeast China during the last 21 ka. *Quaternary Sciences*, *30*(6), 1069–1077. In Chinese with English abstract
- Liu, X., Dong, H., Yang, X., Herzschuh, U., Zhang, E., Stuut, J.-B. W., & Wang, Y. (2009). Late Holocene forcing of the Asian winter and summer monsoon as evidenced by proxy records from the northern Qinghai-Tibetan Plateau. *Earth and Planetary Science Letters*, *280*(1-4), 276–284. <http://doi.org/10.1016/j.epsl.2009.01.041>
- Magny, M., & Haas, J. N. (2004). A major widespread climatic change around 5300 cal. yr BP at the time of the Alpine Iceman. *Journal of Quaternary Science*, *19*(5), 423–430. <https://doi.org/10.1002/jqs.850>
- Magny, M., Leuzinger, U., Bortenschlager, S., & Haas, J. N. (2006). Tripartite climate reversal in Central Europe 5600–5300 years ago. *Quaternary Research*, *65*(01), 3–19. <https://doi.org/10.1016/j.yqres.2005.06.009>
- Mayewski, P. A., Rohling, E. E., Curt Stager, J., Karlén, W., Maasch, K. A., Meeker, L. D., et al. (2004). Holocene climate variability. *Quaternary Research*, *62*(03), 243–255. <https://doi.org/10.1016/j.yqres.2004.07.001>
- Moore, P. D., Webb, J. A., & Collison, M. E. (1991). *Pollen analysis*, (pp. 127–131). Oxford, Great Britain: Blackwell Scientific Publications.
- Moy, C. M., Seltzer, G. O., Rodbell, D. T., & Anderson, D. M. (2002). Variability of El Niño/Southern Oscillation activity at millennial timescales during the Holocene epoch. *Nature*, *420*(6912), 162–165. <https://doi.org/10.1038/nature01194>
- Prentice, I. C., Cramer, W., Harrison, S. P., Leemans, R., Monserud, R. A., & Solomon, A. M. (1992). Special paper: A global biome model based on plant physiology and dominance, soil properties and climate. *Journal of Biogeography*, *19*(2), 117–134. <https://doi.org/10.2307/2845499>
- Press, W. H., Teukolsky, S. A., Flannery, B. P., & Vetterling, W. T. (1992). *Numerical recipes in FORTRAN: The art of scientific computing*, (pp. 95–96). New York, NY, USA: Cambridge University Press.

- Roland, T. P., Daley, T. J., Caseldine, C. J., Charman, D. J., Turney, C. S. M., Amesbury, M. J., et al. (2015). The 5.2 ka climate event: Evidence from stable isotope and multi-proxy palaeoecological peatland records in Ireland. *Quaternary Science Reviews*, *124*(Supplement C), 209–223. <https://doi.org/10.1016/j.quascirev.2015.07.026>
- Sakai, A. (1979). Freezing avoidance mechanism of primordial shoots of conifer buds. *Plant & Cell Physiology*, *20*(7), 1381–1390. <https://doi.org/10.1093/oxfordjournals.pcp.a075937>
- Sakai, A., & Weiser, C. J. (1973). Freezing resistance of trees in North America with reference to tree regions. *Ecology*, *54*(1), 118–126. <https://doi.org/10.2307/1934380>
- Sandweiss, D. H., Maasch, K. A., Burger, R. L., Richardson, J. B., Iii, H., Rollins, B., & Clement, A. (2001). Variation in Holocene El Niño frequencies: Climate records and cultural consequences in ancient Peru. *Geology*, *29*(7), 603–606. [https://doi.org/10.1130/0091-7613\(2001\)029<0603:VIHENO>2.0.CO;2](https://doi.org/10.1130/0091-7613(2001)029<0603:VIHENO>2.0.CO;2)
- Schneider, S. H. (2004). Abrupt non-linear climate change, irreversibility and surprise. *Global Environmental Change*, *14*(3), 245–258. <https://doi.org/10.1016/j.gloenvcha.2004.04.008>
- Sone, T., Kano, A., Okumura, T., Kashiwagi, K., Hori, M., Jiang, X., & Shen, C.-C. (2013). Holocene stalagmite oxygen isotopic record from the Japan Sea side of the Japanese Islands, as a new proxy of the East Asian winter monsoon. *Quaternary Science Reviews*, *75*, 150–160. <http://doi.org/10.1016/j.quascirev.2013.06.019>
- Stebich, M., Rehfeld, K., Schlütz, F., Tarasov, P. E., Liu, J., & Mingram, J. (2015). Holocene vegetation and climate dynamics of NE China based on the pollen record from Sihailongwan Maar Lake. *Quaternary Science Reviews*, *124*, 275–289. <https://doi.org/10.1016/j.quascirev.2015.07.021>
- Steig, E. J. (1999). Mid-Holocene Climate Change. *Science*, *286*(5444), 1485–1487. <https://doi.org/10.1126/science.286.5444.1485>
- Steinhilber, F., Abreu, J. A., Beer, J., Brunner, I., Christl, M., Fischer, H., et al. (2012). 9,400 years of cosmic radiation and solar activity from ice cores and tree rings. *PNAS*, *109*(16), 5967–5971. <https://doi.org/10.1073/pnas.1118965109>
- Steinke, S., Glatz, C., Mohtadi, M., Groeneveld, J., Li, Q., & Jian, Z. (2011). Past dynamics of the East Asian monsoon: No inverse behaviour between the summer and winter monsoon during the Holocene. *Global and Planetary Change*, *78*(3–4), 170–177. <http://doi.org/10.1016/j.gloplacha.2011.06.006>
- Stott, L., Cannariato, K., Thunell, R., Haug, G. H., Koutavas, A., & Lund, S. (2004). Decline of surface temperature and salinity in the western tropical Pacific Ocean in the Holocene epoch. *Nature*, *431*(7004), 56–59. [http://www.nature.com/nature/journal/v431/n7004/supinfo/nature02903\\_S1.html](http://www.nature.com/nature/journal/v431/n7004/supinfo/nature02903_S1.html)
- Stuiver, M., Grootes, P. M., & Braziunas, T. F. (1995). The GISP2  $\delta^{18}\text{O}$  climate record of the past 16,500 years and the role of the Sun, ocean, and volcanoes. *Quaternary Research*, *44*(3), 341–354. <https://doi.org/10.1006/qres.1995.1079>
- Stuiver, M., Reimer, P. J., Bard, E., Beck, J. W., Burr, G. S., Hughen, K. A., et al. (1998). INTCAL98 radiocarbon age calibration, 24,000–0 cal BP. *Radiocarbon*, *40*(03), 1041–1083. <https://doi.org/10.1017/S0033822200019123>
- Sun, C., Liu, Q., Wu, J., Németh, K., Wang, L., Zhao, Y., et al. (2017). The first tephra evidence for a Late Glacial explosive volcanic eruption in the Arxan-Chaihe volcanic field (ACVF), Northeast China. *Quaternary Geochronology*, *40*, 109–119. <https://doi.org/10.1016/j.quageo.2016.10.003>
- Sun, Y., Wang, X., Liu, Q., & Clemens, S. C. (2010). Impacts of post-depositional processes on rapid monsoon signals recorded by the last glacial loess deposits of northern China. *Earth and Planetary Science Letters*, *289*(1–2), 171–179. <http://doi.org/10.1016/j.epsl.2009.10.038>
- Tarasov, P. E., Bezrukova, E. V., & Krivonogov, S. K. (2009). Late glacial and Holocene changes in vegetation cover and climate in southern Siberia derived from a 15 kyr long pollen record from Lake Kotokel. *Climate of the Past*, *5*(3), 285–295. <https://doi.org/10.5194/cp-5-285-2009>
- Torrence, C., & Compo, G. P. (1998). A practical guide to wavelet analysis. *Bulletin of the American Meteorological Society*, *79*(1), 61–78. [https://doi.org/10.1175/1520-0477\(1998\)079<0061:APGTWA>2.0.CO;2](https://doi.org/10.1175/1520-0477(1998)079<0061:APGTWA>2.0.CO;2)
- Wang, B., Wu, R., & Fu, X. (2000). Pacific–East Asian teleconnection: How does ENSO affect East Asian climate? *Journal of Climate*, *13*(9), 1517–1536. [https://doi.org/10.1175/1520-0442\(2000\)013<1517:PEATHD>2.0.CO;2](https://doi.org/10.1175/1520-0442(2000)013<1517:PEATHD>2.0.CO;2)
- Wang, F., Qian, N., & Zhang, Y. (1995). *Pollen morphology of plant in China*. Beijing: Science Press. (In Chinese)
- Wang, H., Prentice, I. C., & Ni, J. (2013). Data-based modelling and environmental sensitivity of vegetation in China. *Biogeosciences*, *10*(9), 5817–5830. <https://doi.org/10.5194/bg-10-5817-2013>
- Wang, K., & Wang, X. (1983). *Palynology outline* (in Chinese). Beijing, China: Peking University Press.
- Wang, L., Li, J., Lu, H., Gu, Z., Rioual, P., Hao, Q., et al. (2012). The East Asian winter monsoon over the last 15,000 years: Its links to high-latitudes and tropical climate systems and complex correlation to the summer monsoon. *Quaternary Science Reviews*, *32*, 131–142. <http://doi.org/10.1016/j.quascirev.2011.11.003>
- Wang, Y., Cheng, H., Edwards, R. L., He, Y., Kong, X., An, Z., et al. (2005). The Holocene Asian monsoon: Links to solar changes and North Atlantic climate. *Science*, *308*(5723), 854–857. <https://doi.org/10.1126/science.1106296>
- Wanner, H., Beer, J., Bütikofer, J., Crowley, T. J., Cubasch, U., Flückiger, J., et al. (2008). Mid-to Late Holocene climate change: an overview. *Quaternary Science Reviews*, *27*(19–20), 1791–1828. <https://doi.org/10.1016/j.quascirev.2008.06.013>
- Wen, C., Graf, H.-F., & Ronghui, H. (2000). The interannual variability of East Asian winter monsoon and its relation to the summer monsoon. *Advances in Atmospheric Sciences*, *17*(1), 48–60. <https://doi.org/10.1007/s00376-000-0042-5>
- Wu, J., & Liu, Q. (2012). Pollen-recorded vegetation and climate changes from Moon Lake since Late Glacial (in Chinese with English abstract). *Earth Science*, *37*(5), 947–954.
- Wu, J., Liu, Q., Wang, L., Chu, G. Q., & Liu, J. Q. (2016). Vegetation and climate change during the last deglaciation in the Great Khingan Mountain, Northeastern China. *PLoS ONE*, *11*(1).
- Wunsch, C. (2006). Abrupt climate change: An alternative view. *Quaternary Research*, *65*(02), 191–203. <https://doi.org/10.1016/j.yqres.2005.10.006>
- Xiao, J., Porter, S. C., An, Z., Kumai, H., & Yoshikawa, S. (1995). Grain size of quartz as an Indicator of winter monsoon strength on the Loess Plateau of Central China during the last 130,000 Yr. *Quaternary Research*, *43*(01), 22–29. <https://doi.org/10.1006/qres.1995.1003>
- Xu, D., Lu, H., Chu, G., Wu, N., Shen, C., Wang, C., & Mao, L. (2014). 500-year climate cycles stacking of recent centennial warming documented in an East Asian pollen record. *Scientific Reports*, *4*(1), 3611.
- Xu, F. J., Li, A. C., & Wan, S. M. (2009). The geological significance of environmental sensitive grain-size populations in the mud wedge of the East China Sea during the mid-Holocene. *Acta Oceanologica Sinica*, *129*(1–2), 229–230.
- Yamamoto, M., Sai, H., Chen, M. T., & Zhao, M. (2013). The East Asian winter monsoon variability in response to precession during the past 150 000 yr. *Climate of the Past*, *9*(6), 2777–2788. <https://doi.org/10.5194/cp-9-2777-2013>
- Zheng, X., Li, A., Wan, S., Jiang, F., Kao, S. J., & Johnson, C. (2014). ITCZ and ENSO pacing on East Asian winter monsoon variation during the Holocene: Sedimentological evidence from the Okinawa Trough. *Journal of Geophysical Research: Oceans*, *119*, 4410–4429. <https://doi.org/10.1002/2013JC009603>

- Zhou, W., Wang, X., Zhou, T. J., Li, C., & Chan, J. C. L. (2007). Interdecadal variability of the relationship between the East Asian winter monsoon and ENSO. *Meteorology and Atmospheric Physics*, *98*(3-4), 283–293. <https://doi.org/10.1007/s00703-007-0263-6>
- Zhou, X., Sun, L., Zhan, T., Huang, W., Zhou, X., Hao, Q., et al. (2016). Time-transgressive onset of the Holocene Optimum in the East Asian monsoon region. *Earth and Planetary Science Letters*, *456*, 39–46. <https://doi.org/10.1016/j.epsl.2016.09.052>
- Zhu, Z., Feinberg, J. M., Xie, S., Bourne, M. D., Huang, C., Hu, C., & Cheng, H. (2017). Holocene ENSO-related cyclic storms recorded by magnetic minerals in speleothems of central China. *Proceedings of the National Academy of Sciences of the United States of America*, *114*(5), 852–857. <https://doi.org/10.1073/pnas.1610930114>